
Article:
Rovira, Carme, Males, Alexandra orcid.org/0000-0002-7250-8300, Davies, Gideon J orcid.org/0000-0002-7343-776X et al. (1 more author) (2020) Mannosidase mechanism : at the intersection of conformation and catalysis. CURRENT OPINION IN STRUCTURAL BIOLOGY. pp. 79-92. ISSN 0959-440X

https://doi.org/10.1016/j.sbi.2019.11.008

Mannosidase mechanism: At the intersection of conformation and catalysis

Carme Rovira,[1,2,*] Alexandra Males,[3] Gideon J. Davies,[3] Spencer J. Williams[4,*]

1 Departament de Química Inorgànica i Orgànica (Secció de Química Orgànica) & Institut de Química Teòrica i Computacional (IQTCUB), Universitat de Barcelona, Martí i Franquès 1, 08028 Barcelona, Spain

2 Institució Catalana de Recerca i Estudis Avançats (ICREA), Pg. Lluís Companys 23, 08010 Barcelona, Spain

3 Department of Chemistry, University of York, Heslington, York YO10 5DD, United Kingdom

4 School of Chemistry and Bio21 Molecular Science and Biotechnology Institute, University of Melbourne, Parkville, Victoria 3010, Australia

sjwill@unimelb.edu.au

Abstract

Mannosidases are a diverse group of enzymes that are important in the biological processing of mannose-containing polysaccharides and complex glycoconjugates. They are found in 12 of the >160 sequence-based glycosidase families. We discuss evidence that nature has evolved a small set of common mechanisms that unite almost all of these mannosidase families. Broadly, mannosidases (and the closely related rhamnosidases) perform catalysis through just two conformations of the oxocarbenium ion-like transition state: a $B_{2,5}$ (or enantiomeric $^{2,5}B$) boat and a $^{3}H_{4}$ half-chair. This extends to a new family (GT108) of GDPMan-dependent β-1,2-mannosyltransferases/phosphorylases that perform mannosyl transfer through a boat conformation as well as some mannosidases that are metalloenzymes and require divalent cations for catalysis. Yet, among this commonality lies diversity. New evidence shows that one unique family (GH99) of mannosidases use an unusual mechanism involving anchimeric assistance via a 1,2-anhydro sugar (epoxide) intermediate.

Introduction

Mannose-containing polysaccharides and glycoconjugates are widespread in nature. For example, β-1,4-mannans are found in a variety of plant sources and include the galactomannans and glucomannans [1]. The cell wall of fungi contain complex heteromannans with an α-1,6-mannan backbone [2] and related structures are present within the lipomannan and lipoarabinomannan structures of mycobacteria and corynebacteria [3]. β-1,2-mannans are produced as a soluble cytosolic carbohydrate reserve in *Leishmania* spp. [4]. And as part of N-linked glycoprotein synthesis, mammals and other eukaryotes produce complex N-glycans that contain β-1,4-, α-1,2-, α-1,3 and α-1,6-mannose linkages. The degradation of these glycosides is achieved by diverse mannosidases (here we use this term to include mannanases) that cleave α- or β-mannoside linkages in a wide variety of substrates. Mannosidases are found within 12 of the glycoside hydrolase families of the Carbohydrate Active enzyme classification (www.cazy.org [5]; www.cazypedia.org [6]). **Table 1** summarizes the various sequence-based families containing mannosidases, and **Table 2** highlights the diversity of fold across the families. Three of these families host α-mannosidase metalloenzymes (and one family hosts α-mannosidase metalloenzymes), with dependency on divalent metals for activity, typically Ca^{2+} or Zn^{2+}.

The chemical transformations used by glycosidases to cleave the glycosidic linkage primarily involve substitution reactions at the anomeric centre of the sugar. Sugars possess a ring oxygen that can provide varying degrees of electronic stabilization to developing charge at C1 and under appropriate conditions the anomeric centre can engage in a continuum of nucleophilic substitution mechanisms that span the spectrum from S_N1 to S_N2 reactions [7●]. The case of a "quintessential" concerted S_N2 reaction at the anomeric position represents one mechanistic extreme, and has only been observed in non-biological catalysis using exceptional nucleophiles (e.g. a glycosyl fluoride with azide) [8] (see **Side panel A**). The other mechanistic extreme involves a "quintessential" stepwise S_N1 reaction with the formation of a glycosyl cation. Glycosyl cations have recently been synthesized in the condensed phase [9], and their involvement as intermediates in non-enzymatic solution-phase glycosylation reactions firmly established [10].

Side panel A. Illuminating the spectrum of reactivity with More O'Ferrall-Jencks plots

More O'Ferrall and Jencks introduced a 2-D plot (which may be contoured to represent energy in the third dimension) that is a useful tool to illustrate the continuity between concerted and stepwise processes. Each axis represents the formation or breakage of a given bond, and a trajectory between substrate at the origin with product at the diagonal illustrates a particular reaction coordinate as a function of changes in bond order for two reactive bonds. More O'Ferrall-Jencks plots are useful to demonstrate the continuity between concerted and stepwise processes such as substitution and elimination reactions. A More O'Ferrall-Jencks plot for an anomeric substitution is shown below. The diagonal represents a perfect S_N2 process, the pathway along the *x*-axis a completely stepwise S_N1 process, and the dotted lines are pathways highlighting the continuum between the two (with dissociative character increasing as the pathway approaches the *x*-axis). The shaded area above the diagonal is excluded for substitution at carbon but may be involved in substitution at phosphorus or sulfur.

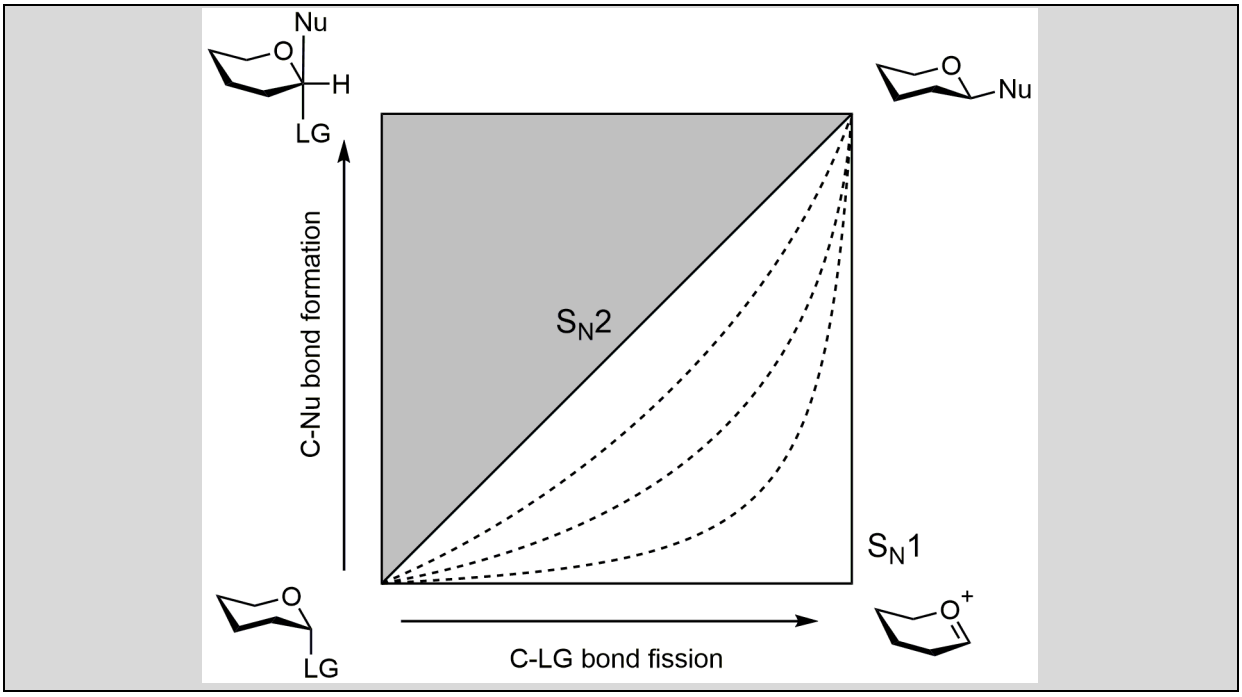

Glycosidases typically possess active sites that stabilize oxocarbenium ion character by favouring certain sugar shapes or conformations [11]. However, in biological catalysis the presence of nucleophilic species within active sites means that glycosyl cations are generally believed not to possess a discrete existence in enzymatic mechanisms [12]. Instead, within enzyme active sites, nucleophilic participation at the anomeric centre is coupled to leaving group departure (dotted lines in **Side panel A**). 'Tight' and 'loose' transition states can be distinguished defined by the sum of the nucleophile…C1 and leaving group…C1 distances [13]. Nonetheless, given the oxocarbenium ion character that develops during glycosidic bond cleavage, the structure and reactivity of glycosyl cations are central to considerations of reactivity in biological catalysis, and provide key insights into the nature of oxocarbenium ion-like transition states. Electronic stabilization of charge development at the transition state results in partial double bond development between O5 and C1 meaning that conformations in which C2-C1-O5-C5 are planar (or close to) are preferred [14]. This includes the idealized half-chair ($^3H_4$, $^4H_3$), boat ($B_{2,5}$, $^{2,5}B$) and envelope (^4E, E_4 and ^3E, E_3) conformations [15].

Glycosidases nominally follow two main nucleophilic substitution mechanisms, distinguished by the stereochemical outcome of the anomeric substitution reaction [14]. Inverting glycosidases operate through one-step mechanisms involving a general acid that assists leaving group departure, and a water nucleophile, assisted by a general base (**Figure 1a,b**). Retaining glycosidases use two-step mechanisms involving a covalent intermediate assisted by an enzymic general acid/base residue [12]. Most retaining glycosidases use an enzyme-borne nucleophile (typically aspartate, glutamate or tyrosine). In the first step the enzyme nucleophile approaches the anomeric centre; coupled to its approach is the departure of the anomeric leaving group, assisted by the enzymic acid/base acting as general acid, resulting in the formation of a covalent glycosyl enzyme (**Figure 1c,d**). In the second step the acid/base acts as general base to deprotonate a water molecule, which substitutes the anomeric centre and cleaves the glycosyl enzyme to restore the enzymatic nucleophile. An important variant of the retaining mechanism applies for substrates bearing a pendant acetamido group situated *trans* to the glycoside, such as *N*-acetyl-β-hexosaminides. Certain *N*-acetyl-β-

hexosamindases utilise a neighboring group participation mechanism in which the substrate acetamido group acts as a nucleophile to displace the leaving group, again with the involvement of an enzymatic general acid/base to promote leaving group departure [12]. These enzymes form a cyclic intermediate that may be either an oxazoline or oxazolinium ion [16●●,17], and possess a general acid/base that both enhances the nucleophilicity of the acetamido group, and stabilizes the oxazolinium ion-like transition state [16●●,18].

In and out of trouble: Nucleophilic substitution of mannosides

Among the range of carbohydrates that nature's catalysts must contend with, polymers and glycoconjugates formed from D-mannose (and its pseudo-enantiomer L-rhamnose) comprise a special case. In mannopyranosides in the normal $^4C_1$ chair conformation, the 2-hydroxyl group occupies an axial orientation. This orientation presents a challenge for nucleophilic substitution reactions at the anomeric position from the β-face. To understand why, one may consider the neopentyl effect (**Figure 2a**): rates of bimolecular S_N2 substitution by ethoxide in neopentyl bromide is around 2,000,000-fold slower than for methyl bromide, more than 150,000-fold slower than for ethyl bromide, and around 4,500-fold slower than the equivalent substitution in isobutyl bromide [19]. The resistance of neopentyl bromide to substitution is credited to blocking of the trajectory required for nucleophilic attack.

Pyranoses can take advantage of their flexibility to relieve the nucleophile blocking effect of the axial 2-hydroxyl and adopt more reactive conformations. The full set of pyranose conformations can be represented using the elegant method of Cremer and Pople [20] using θ/ϕ puckering coordinates on a pseudo-sphere or in 2D in a Mercator projection. In this representation, the 'normal' $^4C_1$ conformation lies at the north pole; the inverted $^1C_4$ conformation at the south pole; the equator consists of various boat and skew conformations; and at the two tropics lie the envelope and half-chair conformations. Varying the ring conformation results in changes to the orientation of O2, which can alleviate the steric clash that occurs as a nucleophile approaches C1, for example by adopting $^OS_2$ or $^3S_1$ conformations (**Figure 2a**). Which conformations are most beneficial for substitutions on mannose C1? Fig 1b shows the degree of 'axiality' of the 2-OH across the conformational orientations, which reveals that the most advantageous are the $^3H_4$ and $B_{2,5}$ conformations; these conformations achieve planarity across C2-C1-O5-C5, and maximize the 'equatoriality' of O2, opening up a nucleophilic trajectory for substitution at C1. Almost all mannosidase Michaelis complexes that have been structurally characterized exhibit pyranose ring conformations in which the 2-hydroxyl is not axial (blue and white regions in **Figure 2b**); family GH99 represents an important exception that will be discussed later.

It has been known since the 1960s that several α-mannosidase (and α-rhamnosidase) families are metalloenzymes that require divalent metal cations (typically Zn^{2+} or Ca^{2+}) for activity (**Table 1**). Cation and substrate bind in that order through an ordered sequential mechanism [21], and X-ray structures reveal that the metal coordinates the 2- and 3-hydroxyls of the substrate. It has been suggested that the role of the metal ion is to assist in distortion of α-mannosides/rhamnosides by effects on the torsion angle of O2-C2-C3-O3 ($\Omega_{O2\text{-}O3}$) [22]. Possibly, for inverting enzymes, the nucleophilic water required in the reaction mechanism is delivered from within the coordination sphere of the metal ion, which may enhance the nucleophilicity of the water by increasing its acidity [22]. A computational study of a GH38 α-mannosidase (a retaining enzyme) argued that Zn^{2+} coordination to the sugar stabilizes charge

development on O2 at the transition state [23], but the effect of the cation on sugar ring conformation was not investigated.

Mannoimidazoles: Privileged probes of transition state conformation

The transition state is the cardinal feature of the catalysis reaction coordinate, but as the least stable species is also the most fleeting. How then can we gain experimental insights into the structure and conformation of the transition state? One approach is to make molecules with the ability to mimic key features of the transition state and use X-ray crystallography to obtain high resolution complexes with enzymes and thereby study the structure and interactions that occur at the transition state. As glycosidases possess a transition state with partial double-bond character and positive charge development at C1 and O5, various sugar-shaped imino/azasugars have proven very useful, especially when validated as transition state mimics through kinetic analysis using Linear Free Energy Relationships on Bartlett plots [24,25]. Prime among the most useful compounds are glycoimidazoles and related species that were developed through the work of Vasella [26] and others. Mannoimidazole especially has emerged as a powerful probe of transition state conformation through a detailed understanding of its intrinsic 'off-enzyme' conformational preferences. The conformational free energy landscape of mannoimidazole determined by quantum mechanical methods revealed that this compound provides good transition-state shape mimicry, with the mechanistically relevant half-chair ($^4H_3$ and $^3H_4$), envelope (^3E, E_3, ^4E, and E_4), and boat ($^{2,5}B$ or $B_{2,5}$) conformations all energetically accessible (**Figure 3**) [27]. The $^4H_3$ conformation is the global minimum, with the $^3H_4$ conformation just 1 kcal mol^{-1} higher in energy. The $B_{2,5}$ conformation is 5 kcal mol^{-1} higher in energy than the $^3H_4$ conformation and it is within the accessible regions of the FEL. Thus, the observation of mannoimidazole bound to enzymes in conformations other than the $^4H_3$ ground state can be considered mechanistically significant, with the enzyme tuning its preferred conformation.

Mannosidases that operate through a $B_{2,5}$ boat conformation

A $B_{2,5}$ transition state conformation for mannosidase catalysis was first proposed based on X-ray structures of a GH26 β-mannanase showing a Michaelis complex in a $^1S_5$ conformation [28], and a glycosyl enzyme formed using a 2-deoxy-2-fluoro-mannoside in a $^OS_2$ conformation [28], suggestive of a boat transition state through application of the principle of least nuclear motion (**Figure 1d**) [15]. This interpolative approach was bolstered by use of a mannobiose-derived imidazole, which bound in a $B_{2,5}$ conformation [27]. $B_{2,5}$ conformations have been observed for mannoimidazole complexes of family GH1, 2, 26, 38, 92, 113, and 125 α- and β-mannosidases (Table 1). In both retaining family GH38 and inverting GH92 α-mannosidases, Zn^{2+}/Ca^{2+} coordinates O2 and O3 in the mannoimidazole complexes [22,27], a feature confirmed by QM/MM simulations of the reaction coordinate features (**Figure 4a**).

The conformational preference of an enzyme has been shown to overcome even greater conformational ligand preferences. A complex of a retaining GH76 enzyme from *Bacillus circulans* with a 1,6-α-mannobiose-derived isofagomine adopted a $B_{2,5}$ conformation [29]. This was surprising as the computed FEL revealed this precise conformer to be approx. 8 kcal mol^{-1} greater than the preferred $^4C_1$ conformation of this inhibitor [27]. QM/MM metadynamics simulation of isofagomine binding to the enzyme revealed that the enzyme dramatically reshapes the FEL to favour the $B_{2,5}$ and $^OS_2$ conformations of this inhibitor on-enzyme, most likely due to a direct hydrogen bonding interactions between the catalytic nucleophile and

inhibitor 3-OH and NH_2^+ groups, allowing the enzyme to qualitatively recapitulate the major hydrogen-bonding interactions predicted for the transition state. Collectively, structural and computational studies support an $^{O}S_2 \rightarrow B_{2,5}^{\ddagger} \rightarrow {}^{1}S_5$ conformational itinerary for the GH76 glycosylation half-reaction (**Figure 1c**).

Family GH1 retaining glycosidases are typically β-glucosidases or β-galactosidases. Cairns and co-workers reported the unusual case of rice Os7BGlu26 β-glycosidase which hydrolyzes 4-nitrophenyl β-glucoside and β-mannoside with similar efficiencies [30]. This is an especially unusual combination as β-glucosidases typically utilize $^{4}H_3$ transition states and β-mannosidases use either $B_{2,5}$ or in rare cases (*vide infra*) $^{3}H_4$ transition states. X-ray structures of glucoimidazole (K_I 2.7 nM) and mannoimidazole (K_I 10.4 μM) revealed that the former binds in a ^{4}E conformation, while the latter binds in a $B_{2,5}$ conformation, suggestive of different transition state conformations for the two substrates. QM/MM simulations supported a $^{1}S_3 \rightarrow {}^{4}E/{}^{4}H_3^{\ddagger} \rightarrow {}^{4}C_1$ itinerary for β-glucosides and a $^{1}S_5 \rightarrow B_{2,5}^{\ddagger} \rightarrow {}^{O}S_2$ itinerary for β-mannosides (**Figure 1d**). Thus, Os7BGlu26 hydrolyzes glucosides and mannosides through distinct pyranoside transition state conformations.

Assignment of the conformational itinerary to the metal-independent family GH125 α-mannosidases has proved challenging. Initial complexes with a non-hydrolysable thiosugar and the iminosugar deoxymannojirimycin were undistorted [31]. Ab initio QM/MM metadynamics of the thiosugar complex but with an S→O replacement performed *in silico* predicted an $^{O}S_2$ conformation on-enzyme [32●●]. This prompted a crystallographic experiment using the acid/base mutant D220N and led to direct observation of an $^{O}S_2$ conformation for the Michaelis complex [32●●]. This was subsequently extended to the observation of a $B_{2,5}$ conformation of mannoimidazole with this enzyme [33], data that collectively supports the assignment of an $^{O}S_2 \rightarrow B_{2,5}^{\ddagger} \rightarrow {}^{1}S_5$ conformational itinerary for GH125 enzymes.

Family GH130 contains β-mannosidases/phosphorylases, both of which act with inversion of stereochemistry. This interesting circumstance arises from two subsets of enzymes that contain either a triad of positively charged (His/Lys/Arg) residues that promote binding of phosphate that can act as the catalytic nucleophile, or instead a pair of glutamates that can activate a water molecule for nucleophilic attack [34]. These enzymes have proven resistant to the obtention of inhibitor complexes. However, various product complexes contain mannose bound in distorted $B_{2,5}$ or $B_{2,5}/{}^{O}S_2$ conformations, and most informatively, Michaelis complexes with disaccharides in which the -1 subsite sugar was bound in a $^{1}S_5$ conformation [35,36]. These data are again collectively consistent with an $^{O}S_2 \rightarrow B_{2,5}^{\ddagger} \rightarrow {}^{1}S_5$ itinerary (**Figures 1d,4b**) [34].

Mannosidases that operate through a $^{3}H_4$ half-chair conformation

α-Mannosidases of family GH47 are inverting and Ca^{2+}-dependent metalloenzymes. The most conspicuous members of this family are the mammalian class I GH47 α-mannosidases involved in N-linked glycoprotein trimming in the secretory pathway in both normal biosynthetic processing and in endoplasmic reticulum associated degradation. A series of X-ray 'snapshots' of an *S*-linked substrate analogue, mannoimidazole, and the product mannose, combined with FEL analysis gave support for a $^{3}S_1 \rightarrow {}^{3}H_4^{\ddagger} \rightarrow {}^{1}C_4$ conformational itinerary (**Figure 1a**) [37,38].

Family 47 α-mannosidases are uniquely sensitive to inhibition to the bicyclic and neutral inhibitor kifunensine, an observation that is exploited in cell biology and in the industrial production of therapeutic proteins [39]. Early crystallographic work applied to mammalian ER α-mannosidase 1 showed that kifunensine adopts an inverted $^{1}C_{4}$ conformation bound to this enzyme [40]. In fact, QM/MM calculations show that kifunensine prefers the ring-flipped $^{1}C_{4}$ conformation over that of the transition state mimicking $^{3}H_{4}$ conformation, which is ~10 kcal mol^{-1} higher in energy and does not correspond to an energy minimum. In the context of the conformational itinerary, this argues that kifunensine achieves its high potency by mimicking the product (rather than the transition state) of the reaction, suggesting that kifunensine achieves selectivity for GH47 mannosidases by its bias to a conformational state that is not accessed by α-mannosidases belonging to other families [41●].

β-Mannanases of family GH134 are inverting glycoside hydrolases that have the capacity to degrade various β-mannans, including unprecedented activity on a challenging substrate, the regular unadorned β-1,4-mannan from the ivory nut [42]. An X-ray structure of mannopentaose complexed with an inactive mutant bacterial GH134 enzyme revealed that the sugar at the –1 subsite adopts a $^{1}C_{4}$ conformation [43]. QM/MM analysis of the reaction coordinate provided evidence for a $^{1}C_{4} \rightarrow {}^{3}H_{4}^{\ddagger} \rightarrow {}^{3}S_{1}$ conformational itinerary (**Figures 1b,4e**). Thus, the GH47 α-mannosidases and the GH134 β-mannanases use the same transition state in equivalent but reversed conformational itineraries for catalysis.

Leishmania β-1,2-mannosyltransferases/phosphorylases: a missing link between GHs and GTs?

Leishmania spp. parasites accumulate a soluble intracellular β-1,2-mannan (mannogen) that functions as a carbohydrate reserve material and confers stability to stress. McConville and co-workers identified a family of enzymes termed β-1,2-mannosyltransferases/phosphorylases (MPTs) that can catalyze the synthesis and degradation of mannogen [44●●]. Five enzymes possess reversible phosphorylic activity, catalysing the stereochemically inverting release of Man-1-phosphate from mannogen (and elongation of mannogen from Man-1-P); two other homologous enzymes catalyzed the reversible extension of mannogen from GDPMan, with the difference in activities associated with an His/Arg switch at a key site within the extended active site cleft that appears to promote phosphate or GDP binding, respectively. The sugar nucleotide transfer activity of this group of enzymes defines them as glycosyltransferases, leading to their assignment to a new family, GT108. However, their ability to act as phosphorylases hints at a connection with the GHs, which in most cases are classified within GH families. Strikingly, X-ray structures of several representatives revealed that they do not adopt one of the typical GT folds, but rather a β-propeller (as predicted for GT91 enzymes), with remarkable similarity of active site with GH130 enzymes that possess β-1,2-mannosidase/phosphorylase activity, including a similar arrangement of catalytic residues. In fact, like enzymes of GH130, a substrate complex with β-1,2-mannobiose was observed with the –1 sugar residue bound in a $^{1}S_{5}$ conformation, and a conformational itinerary $^{1}S_{5} \rightarrow B_{2,5}^{\ddagger} \rightarrow {}^{O}S_{2}$ was proposed, matching that of GH130 β-mannosidases (**Figure 4b,c,d**).

GH family 99 endomannosidase/endomannanases: a new mechanism of glycosidic bond cleavage

Based on observations that can be traced back to the late 19th century it is known that α-mannosides and β-glucosides can be cleaved under basic conditions through a mechanism involving neighboring group participation [45]. These reactions involve the formation of a C2-oxyanion that performs an intramolecular nucleophilic attack on C1 to form a 1,2-epoxide (more formally termed a 1,2-anhydro sugar), which is short-lived under basic conditions, and cleaves through exclusive ring-opening at C1 to form a product with overall stereochemical retention. A recent KIE study of the basic solvolysis of PNPMan revealed a distinctive nucleophile KIE value for C2-^{18}O of 1.04 and anomeric KIEs for anomeric-^{2}H and anomeric 1-^{13}C supporting an oxocarbenium ion-like transition state [45]. As nucleophilic substitution will be preferred when O2 and the anomeric leaving group adopt an antiperiplanar arrangement, this reaction occurs with little requirement for conformational distortion from a $^{4}C_{1}$ conformation with an axial O2. Until very recently proposals for a biological equivalent of this neighboring group participation mechanism by Wallenfels for LacZ β-galactosidase [46,47] and Oppenheimer for NAD^{+} glycohydrolase [48,49,50] have not withstood mechanistic scrutiny.

Glycoside hydrolase family 99 contains retaining enzymes with two closely related activities: *endo*-α-1,2-mannosidases and *endo*-α-1,2-mannanases, which act on corresponding structures present within mammalian glucosylated high mannose N-glycans [51] and yeast mannans [52,53], respectively. An early set of ligand-bound 3-D structures of α-glucosyl-1,3-deoxymannojirimycin and α-glucosyl-1,3-isofagomine complexed to a *Bacteroides* sp. GH family 99 enzyme failed to identify a candidate enzymatic nucleophile, and also did not display any distortion away from a 'normal' $^{4}C_{1}$ conformation [54]. Instead, a conserved carboxylate residue was observed involved in a hydrogen bond with the 2-OH of GlcDMJ and a related inhibitor α-mannosyl-1,3-neoeuromycin [55]. These observations gave indirect support to the suggestion that this family may use a neighboring group participation mechanism involving the 2-OH group via a 1,2-anhydro sugar intermediate [54].

A pre-print available on ChemRxiv reports a non-peer-reviewed study of a *Bacteroides* sp. *endo*-α-1,2-mannanase that yielded a kinetic isotope effects C2-^{18}O of 1.052 ± 0.006 [56●●]. This value is strikingly similar to that measured for the base-promoted solvolysis of PNPMan, and directly supports neighboring group participation by the 2-hydroxyl group. A series of X-ray structures including a tetrasaccharide bound in a Michaelis complex, with cyclohexane-1,2-aziridine and cyclohexane-1,2-epoxide (as mimics of the 1,2-anhydro sugar intermediate) and with mannobiose in a product complex provided insight into the conformations of species along the reaction pathway (**Figure 5**). These structures were used in QM/MM calculations to model the reaction coordinate that also predicted reaction through a 1,2-anhydro sugar intermediate and a $^{2}E/^{2}H_{3} \rightarrow [E_{3}]^{\ddagger} \rightarrow {}^{4}E/^{4}H_{5}$ conformational itinerary. Interestingly, this transition state conformation is very close to the $^{2}H_{3}/E_{3}$ conformation observed upon binding of α-mannosyl-1,3-mannoimidazole (see Fig. 3) [57].

The unique features of this mechanism have inspired the design of activity based protein profiling (ABPP) probes that seek to capitalize on the conserved base that deprotonates O2. Schroder synthesized spiro-epoxides bearing a fluorescent tag that were designed to react with this residue to form a covalent link to the enzyme and allow visualization of the labelled protein [58●]. The best compound (**Figure 5d**) allowed concentration, time and pH dependent visualization of the labelled enzyme after gel electrophoresis, in a manner that could be

competed with by substrate or the inhibitor mannosyl-isofagomine. The Glu333Q and Glu336Q mutant enzymes were not labelled under short labelling conditions that provided effective labelling of the wildtype enzyme, yet were labelled under longer incubation, suggesting that the high reactivity of the spiroepoxide is susceptible to reaction at other sites of the protein and that structural variation may be required to obtain a highly specific ABPP probes suitable for more advanced applications.

Through the looking glass: L-rhamnosidases

Rhamnosidases act on L-rhamnosides, which are the pseudo-enantiomer of D-mannosides. α-L-rhamnoside linkages occur widely in various pectins and the associated degradative enzymes occur within plants and in bacteria in the gut microbiota. All rhamnosidases studied to data process α-L-rhamnosides. Like α-mannosidases, α-rhamnosidases follow inverting and retaining mechanisms, and the rhamnosidases of GH106 are Ca^{2+}-dependent metalloenzymes (Table 1). A complex of a rhamnogalacturonan II degrading bacteroides GH106 α-L-rhamnosidase with L-rhamnotetrazole showed coordination of Ca^{2+} with the 2- and 3-hydroxyl groups and adopted a $^{2,5}B$ conformation [59●●], suggesting that enzymes of this family follow a $^{2}S_{O} \rightarrow {}^{2,5}B^{\ddagger} \rightarrow {}^{5}S_{1}$ conformational itinerary, which is enantiomeric to the $B_{2,5}^{\ddagger}$ pathway followed by most α-mannosidases. Much less is known about the conformational itinerary of all other α-rhamnosidases. Complexes of a GH90 bacteriophage P22 tailspike protein *endo*-rhamnosidase from family GH90 (PDB 1TYU) and *Streptomyces avermitilis* α-rhamnosidase from family GH78 (PDB 3W5N) with rhamnose are found in $^{2,5}B$ conformations hint at a similar conformational itinerary; however, without further study the implications of these observations are unclear. On the basis of a failure to identify a candidate nucleophile for the retaining α-rhamnosidases of GH145, a neighboring group participation mechanism, similar to that of GH99 *endo*-α-1,2-mannanases, was proposed for enzymes of this family [60].

Conclusions

Extensive efforts over the last 20 years combining X-ray crystallography of ligands, kinetic studies and increasingly high-level *ab initio* simulations to the problem of understanding glycoside hydrolase catalysis across the bounty of nature's treasure chest. There is now good evidence that almost all mannosidases follow just two main conformational itineraries involving either a $B_{2,5}^{\ddagger}$ or $^{3}H_{4}^{\ddagger}$ conformation of the transition state. Thus certain α-mannosidases (GH families 38, 76, 125) use an $^{O}S_{2} \rightarrow B_{2,5}^{\ddagger} \rightarrow {}^{1}S_{5}$ itinerary and certain β-mannosidases (GH families 1, 2, 26, 92, 113) and the GH-like GT108 MTPs use a reversed $^{1}S_{5} \rightarrow B_{2,5}^{\ddagger} \rightarrow {}^{O}S_{2}$ itinerary. The first itinerary has also been assigned to GH106 α-rhamnosidases, $^{2}S_{O} \rightarrow {}^{2,5}B^{\ddagger} \rightarrow {}^{5}S_{1}$. Separately, GH family 47 α-mannosidases use a $^{3}S_{1} \rightarrow {}^{3}H_{4}^{\ddagger} \rightarrow {}^{1}C_{4}$ itinerary and GH134 β-mannosidases use the reversed $^{1}C_{4} \rightarrow {}^{3}H_{4}^{\ddagger} \rightarrow {}^{3}S_{1}$ itinerary. This situation is reminiscent of the use of symmetry related $^{1}S_{3} \leftrightarrow {}^{4}H_{3}^{\ddagger} \leftrightarrow {}^{4}C_{1}$ itineraries of α- and β-glucosidases [61].

Nature has finally revealed its closely held secret that the GH99 α-mannosidases operate through a fundamentally distinct mechanism involving neighboring group participation [56●●]. This work demonstrates the that nature can exploit long-established solution phase chemistry to cleave α-mannosides. Unlike classical retaining and inverting mechanisms,

neighboring group participation by the 2-hydroxy group can be considered a specialized rather than a general mechanism that is intrinsically limited to 1,2-*trans* related substrates in which the two groups can readily adopt an antiperiplanar arrangement. Thus, it is not applicable for cleavage of β-mannosides or 2-substituted α-mannosides, and is unlikely to be used for β-glucosides or β-galactosides, which require an energetically costly ring flip to the all (or mostly) axial $^1C_4$ conformation. Possibly, the mechanism may be found to be utilized by α-rhamnosides, which can readily achieve the necessary stereoelectronic arrangement.

The enzymatic control over conformational pathways identified for mannosidases used by nature shares analogy with discoveries made in synthetic chemistry on the effects of bridging protecting groups on controlling access to the flattened oxocarbenium ions invoked in solution phase glycosylation chemistry. The Crich laboratory in particular has utilized 4,6-benzylidene acetals to reduce the stability of mannosyl cations, thereby favouring covalent α-triflates and allowing access to prized β-mannosides [62]. On the other hand, bridging 2,3-*O*-carbonate are argued to (pre)distort the ring and provide easier access to a mannosyl cation and thereby deliver α-mannosides [62]. This latter example presents a clear analogy to one proposed role of O2-O3 coordination by divalent metals in α-mannosidase/α-rhamnosidase metalloenzymes. It is to be hoped that continued investigations into nature's solutions to the problems of biological glycosyl transfer will inspire new solutions to the age-old problem of stereochemical control in chemical glycosylation reactions.

Conflicts of interest

None declared.

Acknowledgements

The Australian Research Council (ARC), the Spanish Ministry of Science, Innovation and Universities (MICINN) and the Agency for Management of University and Research Grants (AGAUR) are thanked for financial support. GJD is supported by the Royal Society through the Ken Murray Research Professorship. We thank Alba Nin-Hill for technical assistance with one of the figures of the manuscript.

References

Papers of particular interest, published within the period of review, have been highlighted as:

● of special interest

●● of outstanding interest

1. Yamabhai M, Sak-Ubol S, Srila W, Haltrich D: **Mannan biotechnology: from biofuels to health**. *Crit. Rev. Biotechnol.* 2016, **36**:32-42.
2. Free SJ: **Fungal cell wall organization and biosynthesis**. *Adv. Gen.* 2013, **81**:33-82.
3. Cao B, Williams SJ: **Chemical approaches for the study of the mycobacterial glycolipids phosphatidylinositol mannosides, lipomannan and lipoarabinomannan**. *Nat. Prod. Rep.* 2010, **27**:919-947.
4. McConville MJ, Naderer T: **Metabolic Pathways Required for the Intracellular Survival of Leishmania**. *Annu. Rev. Microbiol.* 2011, **65**:543-561.
5. Garron ML, Henrissat B: **The continuing expansion of CAZymes and their families**. *Curr. Opin. Chem. Biol.* 2019, **53**:82-87.
6. **Ten years of CAZypedia: a living encyclopedia of carbohydrate-active enzymes**. *Glycobiology* 2018, **28**:3-8.
7. Adero PO, Amarasekara H, Wen P, Bohé L, Crich D: **The Experimental Evidence in Support of Glycosylation Mechanisms at the SN1–SN2 Interface**. *Chem. Rev.* 2018, **118**:8242-8284. ● A major review discussing the evidence for oxocarbenium ions in glycosylation reactions, the factors that influence their formation, and the types of reactive intermediates formed in chemical glycosylation reactions.
8. Chan J, Sannikova N, Tang A, Bennet AJ: **Transition-State Structure for the Quintessential S_N2 Reaction of a Carbohydrate: Reaction of α-Glucopyranosyl Fluoride with Azide Ion in Water**. *J. Am. Chem. Soc.* 2014, **136**:12225-12228.
9. Martin A, Arda A, Désiré J, Martin-Mingot A, Probst N, Sinaÿ P, Jiménez-Barbero J, Thibaudeau S, Blériot Y: **Catching elusive glycosyl cations in a condensed phase with HF/SbF_5 superacid**. *Nat. Chem.* 2015, **8**:186.
10. Hansen T, Lebedel L, Remmerswaal WA, van der Vorm S, Wander DPA, Somers M, Overkleeft HS, Filippov DV, Desire J, Mingot A, et al.: **Defining the S_N1 Side of Glycosylation Reactions: Stereoselectivity of Glycopyranosyl Cations**. *ACS Cent. Sci.* 2019, **5**:781-788.
11. Biarnés X, Nieto J, Planas A, Rovira C: **Substrate Distortion in the Michaelis Complex of *Bacillus* 1,3–1,4-β-Glucanase: Insight from first principles molecular dynamics simulations**. *J. Biol. Chem.* 2006, **281**:1432-1441.
12. Vocadlo DJ, Davies GJ: **Mechanistic insights into glycosidase chemistry**. *Curr. Opin. Chem. Biol.* 2008, **12**:539-555.
13. Schramm VL, Shi W: **Atomic motion in enzymatic reaction coordinates**. *Curr. Opin. Struct. Biol.* 2001, **11**:657-665.
14. Sinnott ML: **Catalytic mechanisms of enzymatic glycosyl transfer**. *Chem. Rev.* 1990, **90**:1171-1202.
15. Speciale G, Thompson AJ, Davies GJ, Williams SJ: **Dissecting conformational contributions to glycosidase catalysis and inhibition**. *Curr. Opin. Struct. Biol.* 2014, **28**:1-13.
16. Coines J, Alfonso-Prieto M, Biarnés X, Planas A, Rovira C: **Oxazoline or Oxazolinium Ion? The Protonation State and Conformation of the Reaction Intermediate of Chitinase Enzymes Revisited**. *Chem. Eur. J.* 2018, **24**:19258-19265. ●● This insightful computational study provides clear evidence that neighboring group participation of a GH18 chitinase proceeds via a neutral oxazoline intermediate.
17. Cekic N, Heinonen JE, Stubbs KA, Roth C, He Y, Bennet AJ, McEachern EJ, Davies GJ, Vocadlo DJ: **Analysis of transition state mimicry by tight binding aminothiazoline inhibitors provides insight into catalysis by human O-GlcNAcase**. *Chem. Sci.* 2016, **7**:3742-3750.

18. Roth C, Petricevic M, John A, Goddard-Borger ED, Davies GJ, Williams SJ: **Structural and mechanistic insights into a *Bacteroides vulgatus* retaining *N*-acetyl-β-galactosaminidase that uses neighbouring group participation**. *Chem. Commun.* 2016, **52**:11096-11099.
19. Hughes ED: **Mechanism and kinetics of substitution at a saturated carbon atom**. *Trans. Faraday Soc.* 1941, **37**:603-631.
20. Cremer D, Pople JA: **General definition of ring puckering coordinates**. *J. Am. Chem. Soc.* 1975, **97**:1354-1358.
21. Nielsen JW, Poulsen NR, Johnsson A, Winther JR, Stipp SL, Willemoës M: **Metal-ion dependent catalytic properties of *Sulfolobus solfataricus* class II α-mannosidase**. *Biochemistry* 2012, **51**:8039-8046.
22. Zhu Y, Suits MDL, Thompson AJ, Chavan S, Dinev Z, Dumon C, Smith N, Moremen K, Xiang Y, Siriwardena A, et al.: **Mechanistic insights into a calcium-dependent family of α-mannosidases in a human gut symbiont**. *Nat. Chem. Biol.* 2010, **6**:125-132.
23. Petersen L, Ardevol A, Rovira C, Reilly PJ: **Molecular mechanism of the glycosylation step catalyzed by Golgi α-mannosidase II: a QM/MM metadynamics investigation**. *J. Am. Chem. Soc.* 2010, **132**:8291-8300.
24. Wicki J, Williams SJ, Withers SG: **Transition-state mimicry by glycosidase inhibitors: a critical kinetic analysis**. *J. Am. Chem. Soc.* 2007, **129**:4530-4531.
25. Tailford LE, Offen WA, Smith NL, Dumon C, Morland C, Gratien J, Heck MP, Stick RV, Bleriot Y, Vasella A, et al.: **Structural and biochemical evidence for a boat-like transition state in β-mannosidases**. *Nat. Chem. Biol.* 2008, **4**:306-312.
26. Heightman TD, Vasella AT: **Recent insights into inhibition, structure and mechanism of configuration retaining glycosidases**. *Angew. Chem. Int. Ed.* 1999, **38**:750-770.
27. Williams RJ, Iglesias-Fernandez J, Stepper J, Jackson A, Thompson AJ, Lowe EC, White JM, Gilbert HJ, Rovira C, Davies GJ, et al.: **Combined inhibitor free-energy landscape and structural analysis reports on the mannosidase conformational coordinate**. *Angew. Chem. Int. Ed.* 2014, **53**:1087-1091.
28. Ducros VM, Zechel DL, Murshudov GN, Gilbert HJ, Szabo L, Stoll D, Withers SG, Davies GJ: **Substrate distortion by a β-mannanase: snapshots of the Michaelis and covalent-intermediate complexes suggest a B(2,5) conformation for the transition state**. *Angew. Chem. Int. Ed.* 2002, **41**:2824-2827.
29. Thompson AJ, Speciale G, Iglesias-Fernandez J, Hakki Z, Belz T, Cartmell A, Spears RJ, Chandler E, Temple MJ, Stepper J, et al.: **Evidence for a boat conformation at the transition state of GH76 α-1,6-mannanases-key enzymes in bacterial and fungal mannoprotein metabolism**. *Angew. Chem. Int. Ed.* 2015, **54**:5378-5382.
30. Tankrathok A, Iglesias-Fernández J, Williams RJ, Pengthaisong S, Baiya S, Hakki Z, Robinson RC, Hrmova M, Rovira C, Williams SJ, et al.: **A single glycosidase harnesses different pyranoside ring transition state conformations for hydrolysis of mannosides and glucosides**. *ACS Catalysis* 2015, **5**:6041-6051.
31. Gregg KJ, Zandberg WF, Hehemann JH, Whitworth GE, Deng L, Vocadlo DJ, Boraston AB: **Analysis of a new family of widely distributed metal-independent α-mannosidases provides unique insight into the processing of N-linked glycans**. *J. Biol. Chem.* 2011, **286**:15586-15596.
32. Alonso-Gil S, Males A, Fernandes PZ, Williams SJ, Davies GJ, Rovira C: **Computational design of experiment unveils the conformational reaction coordinate of GH125 α-mannosidases**. *J. Am. Chem. Soc.* 2017, **139**:1085−1088. ●● Computational QM/MM metadynamics showed that sulfur-for-oxygen substitution in the substrate unfavourably perturbs the energetically-accessible conformational space on-enzyme, allowing design of a crystallographic experiment to access a mechanistically-relevant Michaelis complex.
33. Males A, Speciale G, Williams SJ, Davies GJ: **Distortion of mannoimidazole supports a $B_{2,5}$ boat transition state for the family GH125 α-1,6-mannosidase from *Clostridium perfringens***. *Org. Biomol. Chem.* 2019, **17**:7863-7869.

34. Cuskin F, Basle A, Ladeveze S, Day AM, Gilbert HJ, Davies GJ, Potocki-Veronese G, Lowe EC: **The GH130 Family of Mannoside Phosphorylases Contains Glycoside Hydrolases That Target β-1,2-Mannosidic Linkages in Candida Mannan**. *J. Biol. Chem.* 2015, **290**:25023-25033.
35. Nakae S, Ito S, Higa M, Senoura T, Wasaki J, Hijikata A, Shionyu M, Ito S, Shirai T: **Structure of novel enzyme in mannan biodegradation process 4-O-β-D-mannosyl-D-glucose phosphorylase MGP**. *J. Mol. Biol.* 2013, **425**:4468-4478.
36. Tsuda T, Nihira T, Chiku K, Suzuki E, Arakawa T, Nishimoto M, Kitaoka M, Nakai H, Fushinobu S: **Characterization and crystal structure determination of β-1,2-mannobiose phosphorylase from *Listeria innocua***. *FEBS Lett.* 2015, **589**:3816-3821.
37. Karaveg K, Siriwardena A, Tempel W, Liu Z-J, Glushka J, Wang B-C, Moremen KW: **Mechanism of Class 1 (Glycosylhydrolase Family 47) α-Mannosidases Involved in N-Glycan Processing and Endoplasmic Reticulum Quality Control**. *J. Biol. Chem.* 2005, **280**:16197-16207.
38. Thompson AJ, Dabin J, Iglesias-Fernandez J, Ardevol A, Dinev Z, Williams SJ, Bande O, Siriwardena A, Moreland C, Hu TC, et al.: **The reaction coordinate of a bacterial GH47 α-mannosidase: A combined quantum mechanical and structural approach**. *Angew. Chem. Int. Ed.* 2012, **51**:10997-11001.
39. Cox TM: **Competing for the treasure in exceptions**. *Am. J. Hematol.* 2013, **88**:163-165.
40. Vallée F, Karaveg K, Herscovics A, Moremen KW, Howell PL: **Structural basis for catalysis and inhibition of N-glycan processing class I α-1,2-mannosidases**. *J. Biol. Chem.* 2000, **275**:41287-41298.
41. Males A, Raich L, Williams SJ, Rovira C, Davies GJ: **Conformational analysis of the mannosidase inhibitor kifunensine: a quantum mechanical and structural approach**. *Chembiochem* 2017, **18**:1496-1501. ● This study uses computational methods to define the free energy landscape and show that kifunensine achieves selectivity for GH47 mannosidases by mimicry of the product conformation.
42. Shimizu M, Kaneko Y, Ishihara S, Mochizuki M, Sakai K, Yamada M, Murata S, Itoh E, Yamamoto T, Sugimura Y, et al.: **Novel β-1,4-Mannanase Belonging to a New Glycoside Hydrolase Family in *Aspergillus nidulans***. *J. Biol. Chem.* 2015, **290**:27914-27927.
43. Jin Y, Petricevic M, John A, Raich L, Jenkins H, Portela De Souza L, Cuskin F, Gilbert HJ, Rovira C, Goddard-Borger ED, et al.: **A β-mannanase with a lysozyme-like fold and a novel molecular catalytic mechanism**. *ACS Cent. Sci.* 2016, **2**:896-903.
44. Sernee MF, Ralton JE, Nero TL, Sobala LF, Kloehn J, Vieira-Lara MA, Cobbold SA, Stanton L, Pires DEV, Hanssen E, et al.: **A Family of Dual-Activity Glycosyltransferase-Phosphorylases Mediates Mannogen Turnover and Virulence in *Leishmania* Parasites**. *Cell Host Microbe* 2019, **26**:385-399.e389. ●● Discovery of a new family of glycosyltransferases (GT108) that shares a fold and mechanism with GH130 β-mannoside phosphorylases.
45. Speciale G, Farren-Dai M, Shidmoossavee FS, Williams SJ, Bennet AJ: **C2-Oxyanion neighboring group participation: Transition state structure for the hydroxide-promoted hydrolysis of 4-nitrophenyl α-D-mannopyranoside**. *J. Am. Chem. Soc.* 2016, **138**:14012-14019.
46. Brockhaus M, Dettinger H-M, Kurz G, Lehmann J, Wallenfels K: **Participation of HO-2 in the cleavage of β-D-galactosides by the β-D-galactosidase from *E. coli***. *Carbohydr. Res.* 1979, **69**:264-268.
47. Wallenfels K, Weil R: In *The Enzymes*, edn 3rd Edition. Edited by Boxer PD: Academic Press; 1972:617-663. vol 7.]
48. Egea PF, Muller-Steffner H, Kuhn I, Cakir-Kiefer C, Oppenheimer NJ, Stroud RM, Kellenberger E, Schuber F: **Insights into the Mechanism of Bovine CD38/NAD$^+$ Glycohydrolase from the X-Ray Structures of Its Michaelis Complex and Covalently-Trapped Intermediates**. *PLOS One* 2012, **7**:e34918.
49. Handlon AL, Xu C, Muller-Steffner HM, Schuber F, Oppenheimer NJ: **2'-Ribose Substituent Effects on the Chemical and Enzymic Hydrolysis of NAD+**. *J. Am. Chem. Soc.* 1994, **116**:12087-12088.

50. Johnson RW, Marschner TM, Oppenheimer NJ: **Pyridine nucleotide chemistry. A new mechanism for the hydroxide-catalyzed hydrolysis of the nicotinamide-glycosyl bond**. *J. Am. Chem. Soc.* 1988, **110**:2257-2263.
51. Lubas WA, Spiro RG: **Golgi endo-α-D-mannosidase from rat liver, a novel N-linked carbohydrate unit processing enzyme**. *J. Biol. Chem.* 1987, **262**:3775-3781.
52. Cuskin F, Lowe EC, Temple MJ, Zhu Y, Cameron EA, Pudlo NA, Porter NT, Urs K, Thompson AJ, Cartmell A, et al.: **Human gut Bacteroidetes can utilize yeast mannan through a selfish mechanism**. *Nature* 2015, **517**:165-169.
53. Hakki Z, Thompson AJ, Bellmaine S, Speciale G, Davies GJ, Williams SJ: **Structural and kinetic dissection of the *endo*-α-1,2-mannanase activity of bacterial GH99 glycoside hydrolases from *Bacteroides* spp**. *Chem. Eur. J.* 2015, **21**:1966-1977.
54. Thompson AJ, Williams RJ, Hakki Z, Alonzi DS, Wennekes T, Gloster TM, Songsrirote K, Thomas-Oates JE, Wrodnigg TM, Spreitz J, et al.: **Structural and mechanistic insight into N-glycan processing by endo-α-mannosidase**. *Proc. Natl. Acad. Sci. USA* 2012, **109**:781-786.
55. Petricevic M, Sobala LF, Fernandes P, Raich L, Thompson AJ, Bernardo-Seisdedos G, Millet O, Zhu S, Sollogoub M, Jimenez-Barbero J, et al.: **Contribution of shape and charge to the inhibition of a family GH99 *endo*-α-1,2-mannanase**. *J. Am. Chem. Soc.* 2017, **139**:1089–1097.
56. Sobala LF, Speciale G, Zhu S, Raich L, Sannikova N, Thompson AJ, Hakki Z, Lu D, Shamsi Kazem Abadi S, Lewis AR, et al.: **An Epoxide Intermediate in Glycosidase Catalysis**. *ChemRxiv* 2019, 10.26434/chemrxiv.9745388.v1. ●● This pre-print is a tour de force of structural, mechanistic and computational chemistry and reveals a new mechanism in glycosidase catalysis involving neighboring group participation by the substrate 2-hydroxyl group.
57. Fernandes PZ, Petricevic M, Sobala L, Davies GJ, Williams SJ: **Exploration of Strategies for Mechanism-Based Inhibitor Design for Family GH99 endo-α-1,2-Mannanases**. *Chem. Eur. J.* 2018, **24**:7464-7473.
58. Schroder SP, Kallemeijn WW, Debets MF, Hansen T, Sobala LF, Hakki Z, Williams SJ, Beenakker TJM, Aerts J, van der Marel GA, et al.: **Spiro-epoxyglycosides as Activity-Based Probes for Glycoside Hydrolase Family 99 Endomannosidase/Endomannanase**. *Chem. Eur. J.* 2018, **24**:9983-9992. ● Details the rational design of 2-spiro epoxides as mechanism-based inactivators and evaluation as affinity-based activity probes of family GH99 enzymes.
59. Ndeh D, Rogowski A, Cartmell A, Luis AS, Basle A, Gray J, Venditto I, Briggs J, Zhang X, Labourel A, et al.: **Complex pectin metabolism by gut bacteria reveals novel catalytic functions**. *Nature* 2017, **544**:65-70. ●● This in-depth study of rhamnogalacturonan metabolism by a gut bacterium led to discovery of 7 new glycoside hydrolase families, and predicted the first transition state conformation for an α-rhamnosidase.
60. Munoz-Munoz J, Cartmell A, Terrapon N, Henrissat B, Gilbert HJ: **Unusual active site location and catalytic apparatus in a glycoside hydrolase family**. *Proc. Natl. Acad. Sci. USA* 2017, **114**:4936-4941.
61. Davies GJ, Planas A, Rovira C: **Conformational analyses of the reaction coordinate of glycosidases**. *Acc. Chem. Res.* 2012, **45**:308-316.
62. Crich D: **Mechanism of a Chemical Glycosylation Reaction**. *Acc. Chem. Res.* 2010, **43**:1144-1153.
63. Vincent F, Gloster TM, Macdonald J, Morland C, Stick RV, Dias FMV, Prates JAM, Fontes CMGA, Gilbert HJ, Davies GJ: **Common Inhibition of Both β-Glucosidases and β-Mannosidases by Isofagomine Lactam Reflects Different Conformational Itineraries for Pyranoside Hydrolysis**. *ChemBioChem* 2004, **5**:1596-1599.
64. Helbert W, Poulet L, Drouillard S, Mathieu S, Loiodice M, Couturier M, Lombard V, Terrapon N, Turchetto J, Vincentelli R, et al.: **Discovery of novel carbohydrate-active enzymes through the rational exploration of the protein sequences space**. *Proc. Natl. Acad. Sci. USA* 2019, **116**:6063-6068.

Table 1. Conformational itineraries, mechanisms and metal-dependency assigned to mannosidases from various glycoside hydrolase families

Enzyme	Families	Stereochemistry	Conformational itinerary
α-mannosidase	**38*** [27], **76** [29]	retaining	${}^{O}S_2 \rightarrow B_{2,5}^{\ddagger} \rightarrow {}^{1}S_5$
	92* [22], **125** [32●●,33]	inverting	${}^{O}S_2 \rightarrow B_{2,5}^{\ddagger} \rightarrow {}^{1}S_5$
	47* [38]	inverting	${}^{3}S_1 \rightarrow {}^{3}H_4^{\ddagger} \rightarrow {}^{1}C_4$
	99	retaining	${}^{2}E/{}^{2}H_3 \rightarrow [E_3]^{\ddagger} \rightarrow {}^{4}E/{}^{4}H_5$
β-mannosidase	**1** [30], **2** [25], **5** [63], **26** [27,28], **113** [27], **130** [34]	retaining	${}^{1}S_5 \rightarrow B_{2,5}^{\ddagger} \rightarrow {}^{O}S_2$
	134 [43]	inverting	${}^{1}C_4 \rightarrow {}^{3}H_4^{\ddagger} \rightarrow {}^{3}S_1$
	164** [64]	unknown	unknown
α-rhamnosidase	**145**	retaining	unknown
	106* [59●●]	inverting	${}^{2}S_O \rightarrow {}^{2,5}B^{\ddagger} \rightarrow {}^{5}S_1$
	28, **78**, **90**	inverting	unknown

* GH metalloenzymes using divalent metals.

**Following correspondence from one of us (GJD) this enzyme family activity was reassigned as β-mannosidase.

Table 2. The structural diversity of mannosidases (and the mannosidase-like family GT108).

Families	Fold	Metal centre
1, 2, 5, 26, 99, 113	$(\alpha/\beta)_8$ barrel	–
28, 90	β-helix	–
38	large globular domain: αβ region and all β region	Zn^{2+} site in the αβ region
47	$(\alpha/\alpha)_7$ barrel	Ca^{2+} site at base of barrel, plugged by β-hairpin
92	N-terminal β-sandwich C-terminal $(\alpha/\alpha)_6$ barrel	Ca^{2+} site at base of $(\alpha/\alpha)_6$ barrel, facing β-sandwich domain
106	$(\alpha/\beta)_8$ barrel catalytic domain interrupted with three β-sandwich domains and appended with C-terminal β-sandwich domain	Ca^{2+} site at top of $(\alpha/b)_8$ barrel,
78, 125	$(\alpha/\alpha)_6$ barrel	–
130	5-bladed β-propeller	–
134, GT108	lysozyme fold	–
145	7-bladed β-propeller	–
164	unknown	–

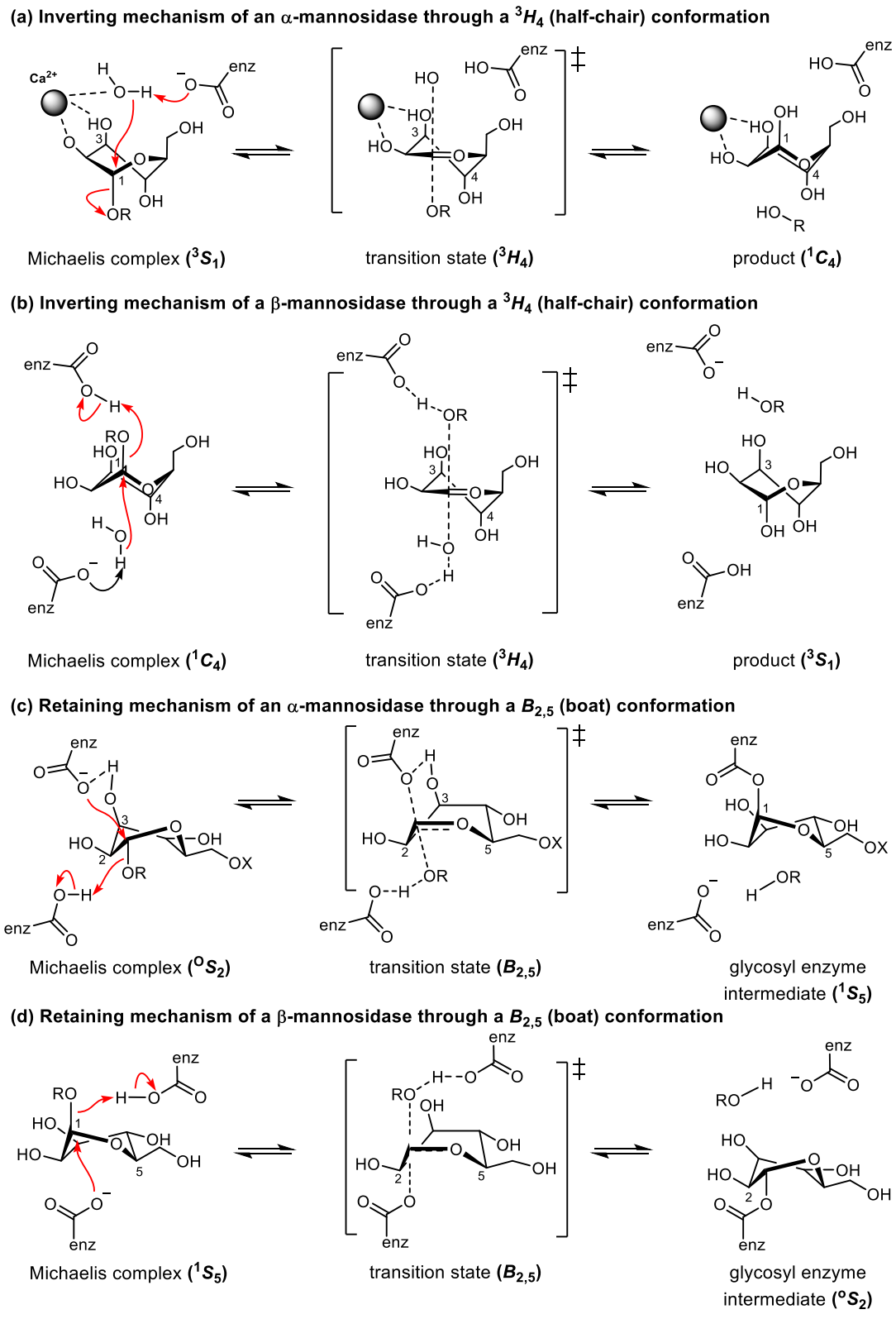

Figure 1. Mechanisms for **(a,b)** inverting α-mannosidases (GH47) and β-mannosidases (GH134) that proceed through a $^3H_4$ transition state conformation, and **(c,d)** glycosylation half-reaction of retaining α-mannosidases (GH38, 76) and β-mannosidases (GH1, 2, 5, 26, 113) that proceed through a $B_{2,5}$ transition state conformation (GH38 retaining α-mannosidases and GH92 inverting α-mannosidases follow similar mechanisms but are metal dependent).

(a) Blocked nucleophilic trajectories in mannose can be alleviated by conformational distortion

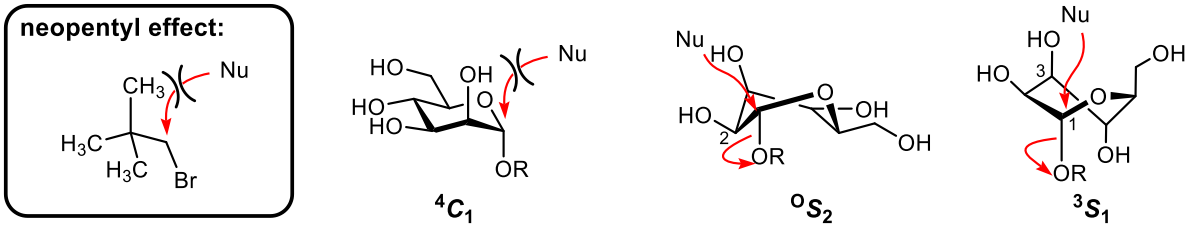

(b) O2-Axiality plot for mannose across the Cremer-Pople coordinates

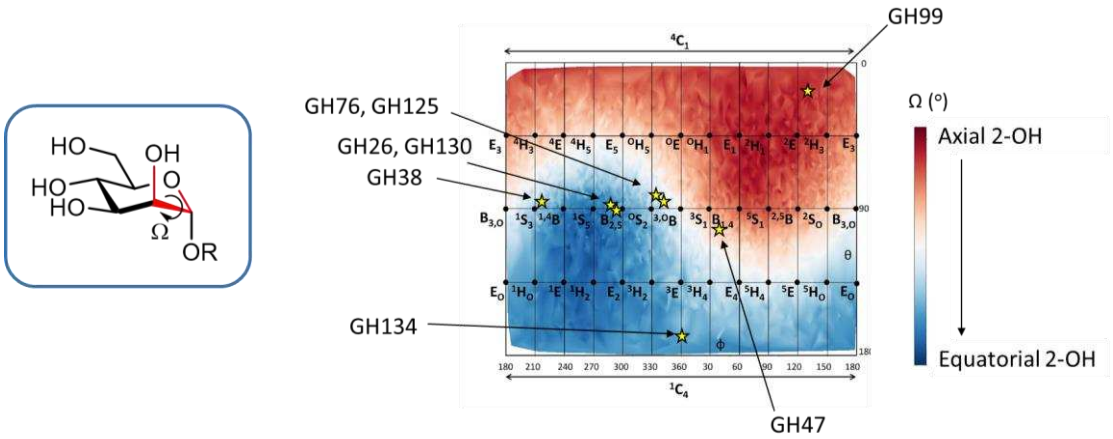

(c) Ligands

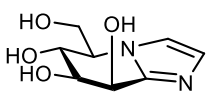

mannoimidazole

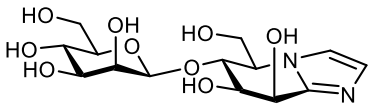

β-mannosyl-1,4-mannoimidazole

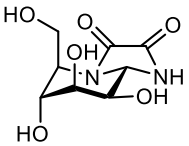

kifunensine

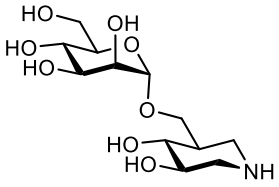

α-mannosyl-1,6-isofagomine

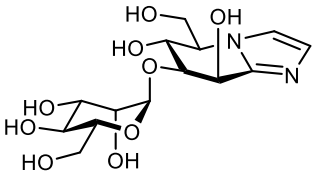

α-mannosyl-1,3-mannoimidazole

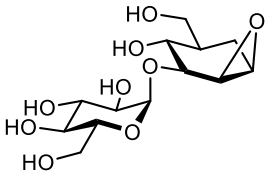

α-glucosyl-1,3-cyclohexane epoxide

Figure 2. (a) Nucleophilic attack on an α-mannoside in a $^4C_1$ conformation suffers from a 1,2-diaxial interaction that interrupts the nucleophilic trajectory, analogous to the neopentyl effect. This effect can be relieved by conformational distortion to an $^OS_2$ or $^4H_3$ conformation. **(b)** Plot showing O2 axial/equatorial percentage across the Cremer-Pople conformational landscape, and with the conformation of the individual family representatives from PDB files of X-ray structures of Michaelis or intermediate complexes indicated with stars (GH26 1GVY; GH38 1QX1; GH47 4AYP; GH76 5AGD; GH125 5M7Y; GH130 5B0R; GH134 5JUG [38]. **(c)** Ligands discussed in this article.

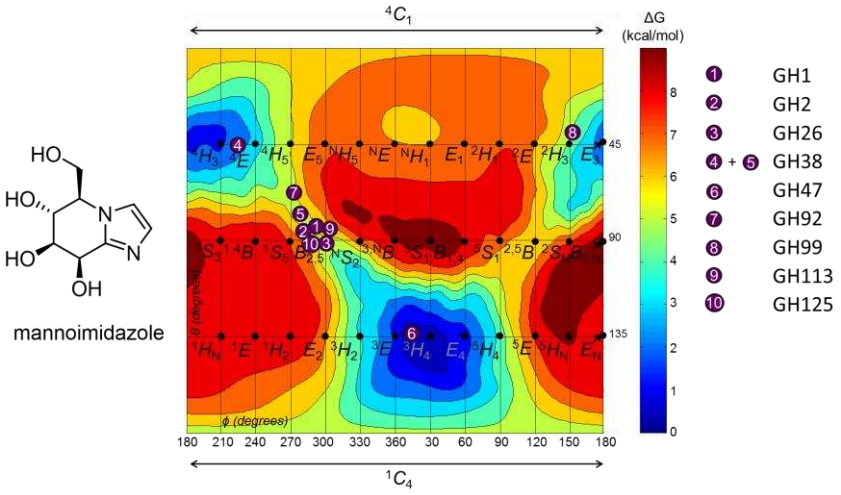

Figure 3. Free energy landscape for mannoimidazole, with coordinates for the observed conformation of mannoimidazole-type ligands in the –1 subsite for enzymes from families **(1)** GH1 (PDB 4RE2), **(2)** GH2 (PDB 2VMF), **(3)** GH26 (PDB 4CD5), **(4)**+**(5)** GH38 (PDB 3D4Y), **(6)** GH47 (PDB 4AYQ), **(7)** GH92 (PDB 2WZS), **(8)** GH99 (PDB 6FAR), **(9)** GH113 (PDB 4CD8), **(10)** GH125 (PDB 6RQK).

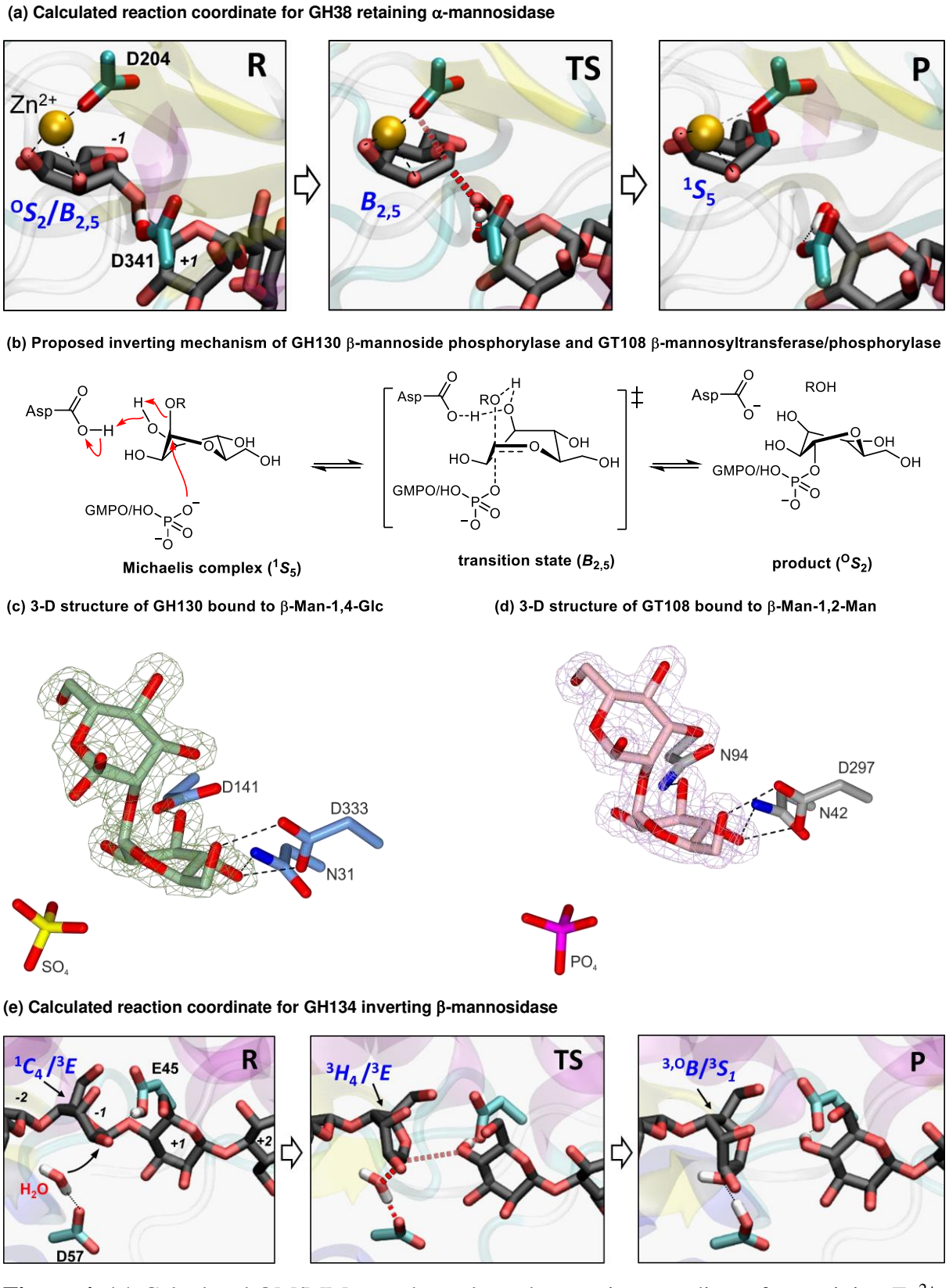

Figure 4. **(a)** Calculated QM/MM snapshots along the reaction coordinate for retaining Zn^{2+}-dependent family GH38 α-mannosidase, via a transition state in a $B_{2,5}$ conformation [23]. **(b)** Inverting mechanism proposed for GH130 β-mannoside phosphorylases and GT108 β-mannosyltransferase/phosphorylases, showing participation of the 3-hydroxyl. **(b)** 3-D structure of β-Man-1,2-Man (green) complex of *Listeria innocua* β-1,2-mannobiose

phosphorylase (blue) showing substrate in a $^{1}S_{5}$ conformation and sulfate location (yellow). $2mF_o$-F_c weighted electron density map (dark green) contoured at 1.0 $e^-/Å^3$. D141 is the putative general acid catalyst. **(c)** 3-D structure of β-Man-1,2-Man (pink) complex of *Leishmania mexicana* β-mannosyltransferase/phosphorylase MPT2 D94N mutant (grey) showing substrate in a $^{1}S_{5}$ conformation, superposed with the phosphate location (magenta) from the homologous MTP4 structure. $2mF_o$-F_c weighted electron density map (light pink) contoured at 0.5 $e^-/Å^3$. **(e)** Calculated QM/MM snapshots along the reaction coordinate for inverting family GH134 β-mannosidase, via a transition state in a $^{3}H_{4}$ conformation [43].

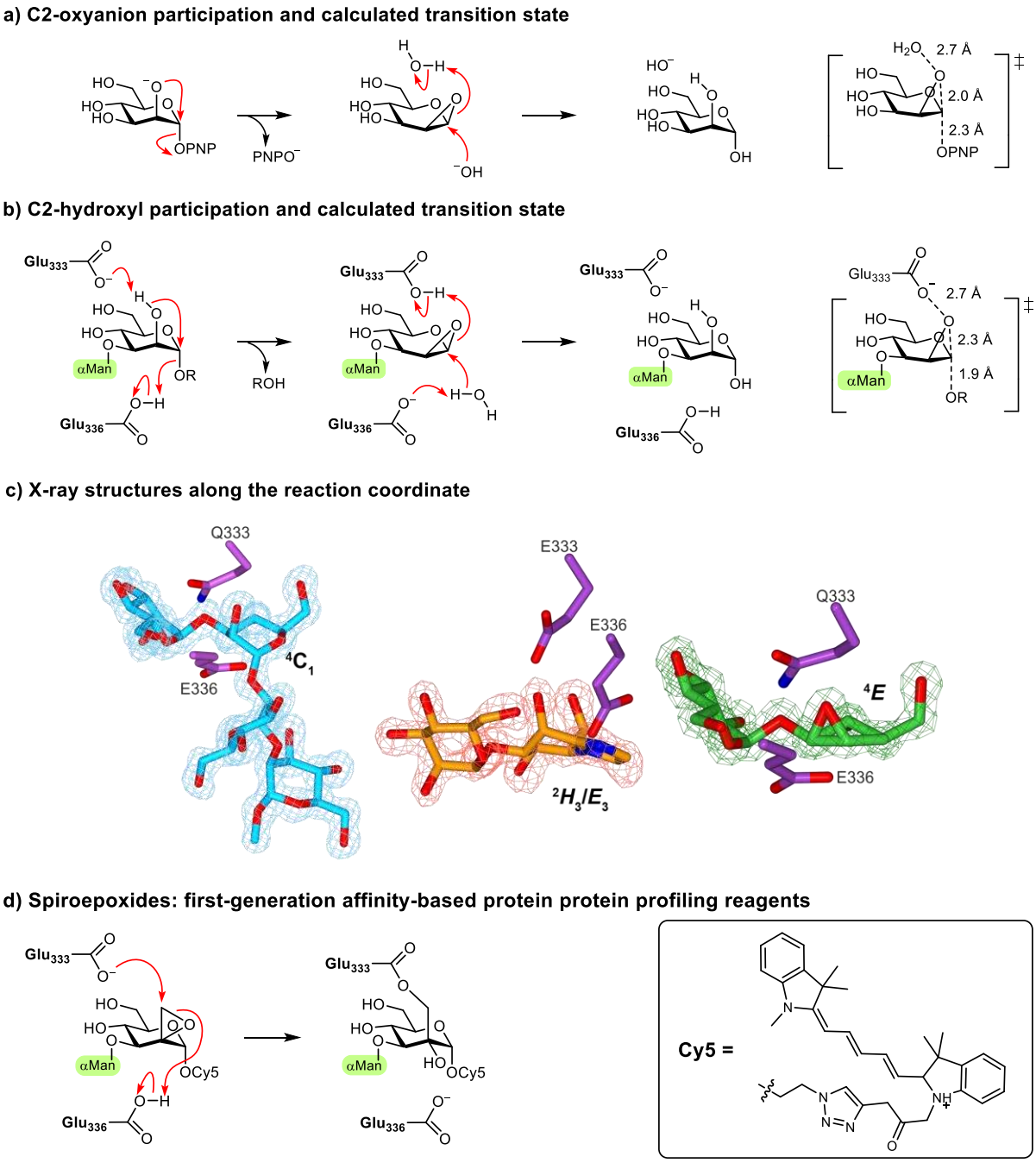

Figure 5. Neighboring group participation by the 2-hydroxyl of α-mannosides. **(a)** Mechanism for neighboring group participation by a C2-oxyanion in the base-mediated solvolysis of 4-nirophenyl α-D-mannopyranoside (PNPMan). Right: ab initio calculated interatomic distances for the critical interactions at the solvolytic transition state [45]. **(b)** Mechanism for neighboring group participation by family GH99 *endo*-α-1,2-mannanase. Right: QM/MM calculation of interatomic distances for the critical interactions at the enzymatic transition state [56●●]. **(c)** Snapshots along the reaction coordinate: Michaelis complex with α-Man-1,3-α-Man-1,2-α-Man-1,2-α-Man-OMe [56●●], α-mannosyl-1,3-mannoimidazole [57] and α-glucosyl-1,3-cyclohexane-β-1,2-epoxide [56●●]. **(d)** Spiroepoxides have been reported as first-generation affinity-based protein profiling reagents, designed based on the epoxide intermediate *endo*-α-1,2-mannanase mechanism [58●].

Conflicts of interest

No conflicts of interest to declare